Electronic Supplementary Material (ESI) for Journal of Materials Chemistry A.

Supplementary Information

In-situ encapsulate Fe_3O_4 nanosheet arrays with graphene layers as anode for high-performance asymmetric supercapacitors

Jinghuang Lin[1], Haoyan Liang[1], Henan Jia[1], Shulin Chen[1], Jiale Guo[1], Junlei Qi*[1], Chaoqun Qu[2], Jian Cao*[1], Weidong Fei[1] and Jicai Feng[1]

1. State Key Laboratory of Advanced Welding and Joining, Harbin Institute of Technology, Harbin 150001, China

2. Key Laboratory of Functional Materials Physics and Chemistry of the Ministry of Education, Jilin Normal University, Siping 136000, China

*Corresponding authors: Tel. /fax: 86-451-86418146;

E-mail: jlqi@hit.edu.cn (J. Qi)

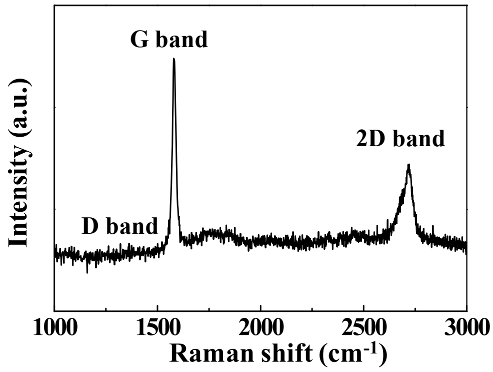

Fig. S1 Raman spectrum of g-Ni foam.

As shown in Fig. S1, it can be found that the g-Ni foam showed the weak D band at about 1350 cm^{-1}. It suggested that the synthesized graphene on Ni foams possessed a high degree of graphitization [53].

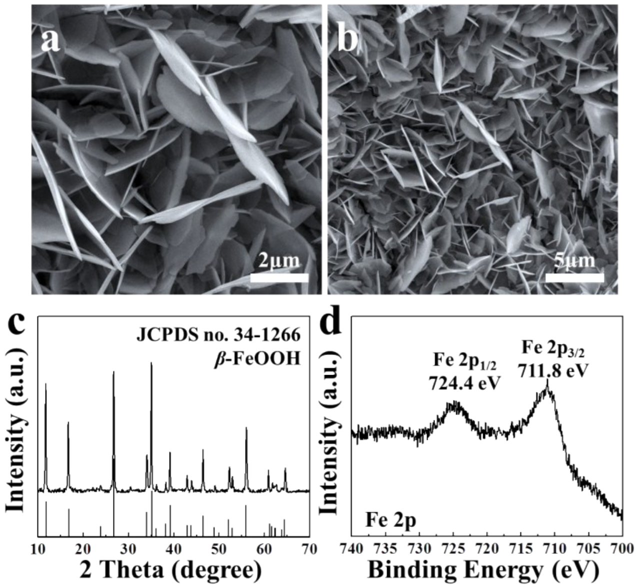

Fig. S2 (a, b) SEM images, (c) XRD pattern and (d) XPS Fe 2p spectrum of the FeOOH nanosheets.

The SEM images in Fig. S2a and S2b reveal that FeOOH nanosheets were vertically grown on the substrates. The XRD pattern in Fig. S2c confirms these nanosheets consist of β-FeOOH (JCPDS No. 34-1266) [51]. The high-resolution Fe 2p in Fig. S2d also confirm the existence of β-FeOOH [52], which is consistent with XRD results.

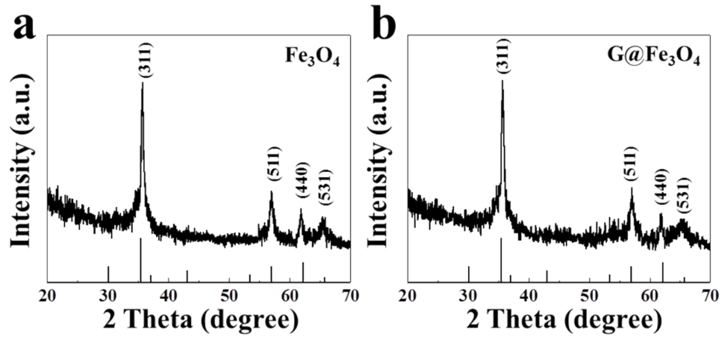

Fig. S3 XRD patterns of (a) Fe_3O_4 and (b) G@Fe_3O_4 samples separated from the substrates.

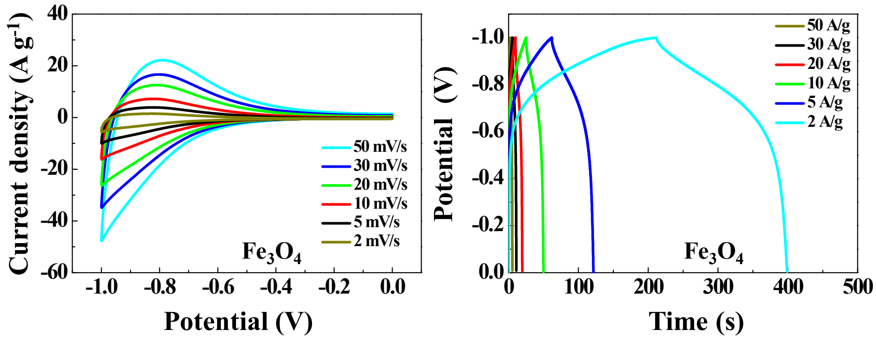

Fig. S4 (a) CV and (b) GCD curves of Fe_3O_4 electrode.

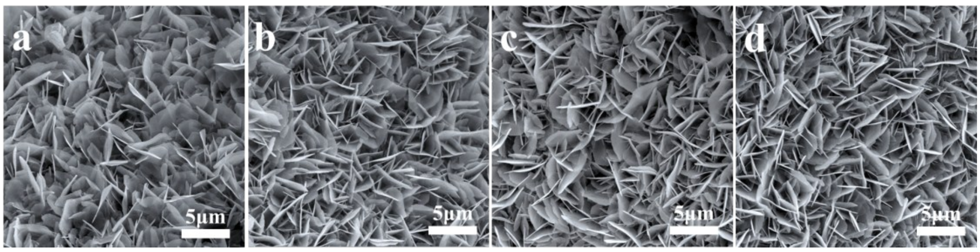

Fig. S5 SEM images of (a) G@Fe_3O_4-0.5, (b) G@Fe_3O_4-1, (c) G@Fe_3O_4-3 and (d) G@Fe_3O_4-5

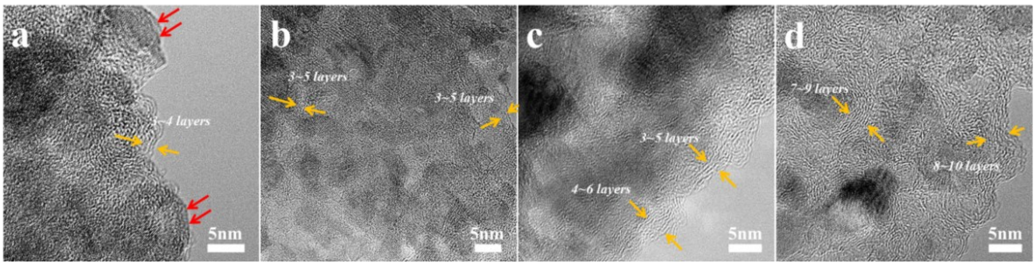

Fig. S6 HRTEM images of (a) G@Fe_3O_4-0.5, (b) G@Fe_3O_4-1, (c) G@Fe_3O_4-3 and (d) G@Fe_3O_4-5

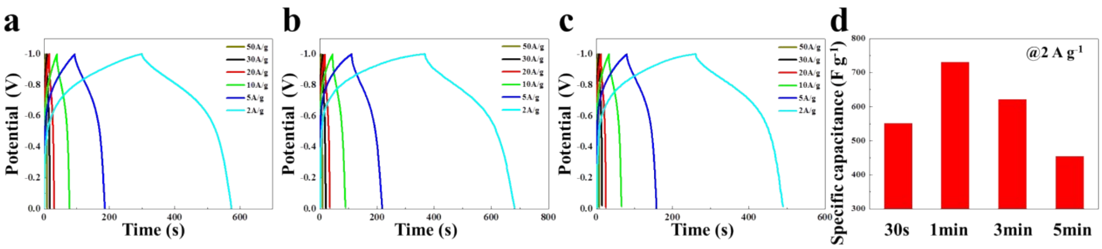

Fig. S7 GCD curves of (a) G@Fe_3O_4-0.5, (b) G@Fe_3O_4-3 and (c) G@Fe_3O_4-5. (d) The calculated capacitances of G@Fe_3O_4 with different deposition time at 2 A g^{-1}.

In order to optimize the synthetic conditions, we conducted PECVD process for 0.5 min, 1 min, 3 min and 5 min to obtain different samples (briefly named as G@Fe_3O_4-0.5, G@Fe_3O_4-1, G@Fe_3O_4-3 and G@Fe_3O_4-5). As shown in Fig. S5, it can be found that G@Fe_3O_4 samples maintained the nanosheet morphology. Fig. S6a-S6d show the HRTEM images of G@Fe_3O_4-0.5, G@Fe_3O_4-1, G@Fe_3O_4-3 and G@Fe_3O_4-5, respectively. As shown in Fig. s6a, it can be found that the G@Fe_3O_4-0.5 is covered with about 3~4 layers of graphene. However, some parts of G@Fe_3O_4-0.5 are uncovered with graphene (marked with red arrows), which may be due to the short time deposition process. As the deposition time prolong, the graphene layers is gradually increased. It is worth noting that G@Fe_3O_4-5 are covered with thick graphene layer (7~10 layers). According to the previous researches [54,55], moderate graphene layers with high crystallinity nature are favorable for improving the electronic conductivity, mechanical properties, and electrochemical performance of G@Fe_3O_4 samples. Fig. S7a-S7c show the GCD curves of G@Fe_3O_4-0.5, G@Fe_3O_4-3 and G@Fe_3O_4-5, respectively. Based on GCD curves, the calculated capacitances are shown in Fig. S7d. It can be found that the maximum capacitance reached to 732 F g^{-1} for G@Fe_3O_4-1 samples. Thus, we choose the optimized deposition time is 1 min. The long time deposition can lead to the thick graphene layers on Fe_3O_4, which would access to a downward trend of specific capacitance of G@Fe_3O_4 samples. Obviously, encapsulating superabundant graphene layers on Fe_3O_4 has a negative effect on electrode performance G@Fe_3O_4, mainly because of the sacrifice of contact area between Fe_3O_4 and electrolyte. Undoubtedly, it suggested that moderate graphene layers can improve the electrochemical performances of Fe_3O_4 samples.

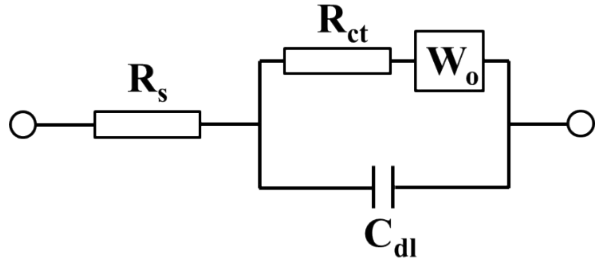

Fig. S8 The AC impedance equivalent circuit.

As shown in Fig. S8, R_{ct} represents the charge transfer resistance, which can be estimated by the diameter of the semicircle in the high-frequency region. R_s, W_o and C_{dl} represent the bulk resistance, Warburg diffusion resistance and double layer capacitance, respectively [56-58].

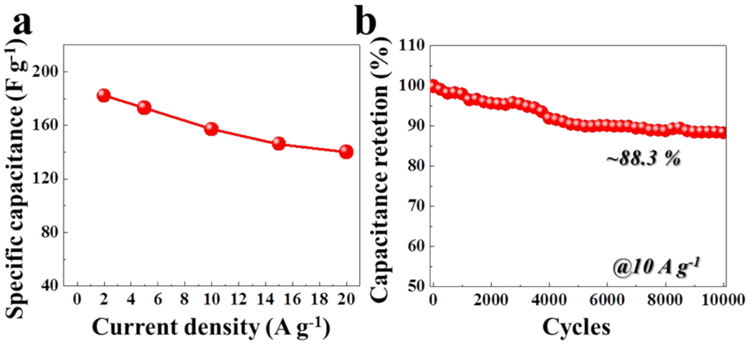

Fig. S9 (a) The calculated specific capacitance of ASCs. (b) Cycling stability at 10 A g^{-1} of ASCs.

Table S1. The specific capacitance of various electrodes in the three-electrode system in references

electrode materials	electrolyte	potential window	specific capacitance	reference
Fe_3O_4 nanosheets	2 M KOH	-1~0 V	379.8 F g^{-1}	1
Fe_2O_3 nanotube	1 M Li_2SO_4	-0.8~0.1 V	300.1 F g^{-1}	3
Fe_2O_3@C nanoparticles	1 M Na_2SO_4	-0.5~0.5 V	211.4 F g^{-1}	4
3D-KSPC/Fe_3O_4-DCN	2 M KOH	-0.8~0.2 V	285.4 F g^{-1}	5
Fe_2O_3 nano-dots@N-dope graphene	2 M KOH	-1.0~0 V	274 F g^{-1}	7
Fe_3O_4@FLG/PEDOT:PSS	0.5M Na_2SO_3	-1.3~-0.4V	153 F g^{-1}	8
hollow and porous Fe_2O_3	0.5M Na_2SO_3	-1.0~-0.1V	346 F g^{-1}	9
NiNTAs@Fe_2O_3 nanoneedles	1 M Na_2SO_4	-0.8-0 V	418.7 F g^{-1}	10

particle-exfoliated graphite/Fe_3O_4	1 M KOH	-1.1~0 V	327 F g^{-1}	11
Fe_3O_4/carbon nanotube/polyaniline ternary films	2 M KOH	-0.5~0.5 V	201 F g^{-1}	13
Fe_3O_4 nanoparticles//rGO	1M KOH	-1~0 V	241 Fg^{-1}	14
3D Fe_3O_4/rGO	2 M KOH	-1.0~0.4 V	455 F g^{-1}	15
Fe_3O_4/carbon hybrid nanoparticles	1MNa_2SO_3	-0.6~0.3 V	455 F g^{-1}	26
Fe_3O_4/carbon nanofibres	3 M KOH	-1.05~-0.35V	225 F g^{-1}	27
monodisperse Fe_3O_4 nanoparticles/graphene	1 M KOH	-1~0 V	368 F g^{-1}	28
Fe_3O_4/rGO	1 M LiOH	-1.15~0.1 V	326 F g^{-1}	29.
Fe_3O_4/CNTs	6 M KOH	-1.0~0 V	129 F g^{-1}	30
Fe_2O_3 QD/FGS	1 M Na_2SO_4	-1.0~0 V	347 F g^{-1}	31
α-Fe_2O_3/graphene	1 M Na_2SO_4	-1.0~0 V	504 F g^{-1}	32
FeOOH quantum dots	1 M Li_2SO_4	-0.8~0 V	365 F g^{-1}	33
Fe_3O_4@Fe_2O_3 Nanorod	1 M Na_2SO_4	-1.0~0 V	231.9 F g^{-1}	34
Ti-doped Fe_2O_3@PEDOT	5 M LiCl	-0.8~0 V	311.6 F g^{-1}	35
α-Fe_2O_3/carbon nanotube sponges	2 M LiCl	-1.0~0 V	296.3 F g^{-1}	36
G@Fe_3O_4	2 M KOH	-1.0~0 V	732 F g^{-1}	This work

Table S2. Comparison of the electrochemical performance of as-fabricated ASC device with those in previous reports.

Asymmetric supercapacitor	**C_{cell} (F g^{-1})**	**Energy density (Wh kg^{-1})**	**Corresponding Power density (W kg^{-1})**	**Reference**
Co_2AlO_4@MnO_2//Fe_3O_4	99.1	35.25	800.1	1
MnO_2//Fe_2O_3@PPy	94.2	42.4	268.8	6
NiNTAs@MnO_2//NiNTAs@Fe_2O_3	95.9	34.1	3197.7	10
Ni-Co double hydroxide// particle-exfoliated graphite/Fe_3O_4	124.2	54	876	11
multishelled NiO hollow microspheres//	143.4	51.0	800	12

RGO@Fe_3O_4				
$NiCo_2S_4$//Fe_2O_3	124.8	44.4	1620	16
MoS_2-NiO//MoS_2-Fe_2O_3	111.4	39.6	807.2	17
$NiGa_2S_4$ microspheres//N,S-codoped graphene/Fe_2O_3	123	43.6	961	18
$CoMoO_4$@$NiMoO_4\cdot xH_2O$//Fe_2O_3	153.6	41.8	700	19
NiCoP nanoplates//graphene film	105.3	32.9	1301	20
oxygen-deficient Co_3O_4//AC	60.3	24.2	600	21
$MnCo_2O_4$@$Ni(OH)_2$//AC	141	48	1400	22
Co_3O_4 nanosheets//MnO@C nanosheets	166	59.6	1529.8	23
CNFs@$ZnCo_2O_4$//CNFs	139.2	49.5	222.7	24
$NiMoO_4$//AC	151.7	60.9	850	25
Ni-Co-S//porous graphene	133	60	1800	37
$NiCo_2S_4$/Ni_3S_2//rGO	175	62.2	800	38
$ZnCo_2O_4$@$Ni_xCo_{2x}(OH)_{6x}$//AC	65.3	26.2	511.8	39
$CuCo_2O_4$/CuO//RGO/Fe_2O_3	93	33.0	200	40
$CuCo_2S_4$//AC	124	44.1	800	41
$CuCo_2O_4$/NiO//AC	155	51.8	866	42
MnCo-LDH@$Ni(OH)_2$//AC	152	47.6	750.7	43
Ni-Co-S/graphene//carbon nanosheets	122	43.3	800	44
Meso-NiO/Ni//carbon nanocage	53.7	19.1	700	45
CC@Co_3O_4//CC@NC	116.8	41.5	6200	46
NiO@FeCo-LDH//pen ink/graphene/carbon nanotube	205	64.1	1500	47
MnNi LDH@VG//AC	160	56.8	260	48
Co(P,S) nanotubes//CC	109.5	39	800	49
onion-like $NiCo_2S_4$ particles//AC	120	42.7	1583	50
H-TiO_2@$Ni(OH)_2$//N–C	150.6	70.9	102.9	59
$CuCo_2O_4$//G@Fe_3O_4	182	82.8	2047	This work

References

1. F. Li, H. Chao, X. Liu, J. Jia, C. Xu, F. Dong, Z. Wen, Y. Zhang, J. Mater. Chem. A 4 (2016) 2096-2104.

2. C. Guan, J. Liu, Y. Wang, L. Mao, Z. Fan, Z. Shen, H. Zhang, J. Wang, ACS Nano 9 (2015) 5198-5207.

3. Y. Liu, Y. Hsu, Y. Lin, Y. Chen, Electrochim. Acta 216 (2016) 287-294.

4. M. Zhang, J. Sha, X. Miao, E. Liu, C. Shi, J. Li, C. He, Q. Li, N, Zhao, J. Alloys Compd. 696 (2017) 956-963.

5. L. Wang, J. Yu, X. Dong, X. Li, Y. Xie, S. Chen, P. Li, H. Hou, Y. Song, ACS Sustain. Chem. Eng. 4 (2016) 1531-1537.

6. P. Tang, L. Han, A. Genç, Y. He, X. Zhang, L. Zhang, J. R. Galán-Mascarós, J. R. Morante, J. Arbiol, Nano Energy, 22 (2016) 189-201.

7. L. Liu, J. Lang, P. Zhang, B. Hu, X. Yan, ACS Appl. Mater. Interfaces 8 (2016) 9335-9344.

8. E. Pardieu, S. Pronkin, M. Doici, T. Dintzer, B. P. Pichon, D. Begin, C. Pham-Huu, P. Schaaf, S. Begin-Colin, F. Boulmedais, J. Mater. Chem. A 3(2015) 22877-22885.

9. C. Fu, A. Mahadevegowda, P.S. Grant, J. Mater. Chem. A 4 (2016) 2597-2604.

10. Y. Li, J. Xu, T. Feng, Q. Yao, J. Xie, H. Xia, Adv. Funct. Mater. 27 (2017) 1606728.

11. Z. Sun, X. Cai, Y. Song, X. Liu, J. Power Sources 359 (2017) 57-63.

12. X.H. Qi, W. J. Zheng, X. Li, G. He, Sci. Rep. 6 (2016) 33241.

13. J. Li, W. Lu, Y. Yan, T. Chou, J. Mater. Chem. A 5 (2017) 11271-11277.

14. L. Li, P. Gao, S. Gai, F. He, Y. Chen, M. Zhang, P. Yang, Electrochim. Acta 190 (2016) 566-573.

15. R. Kumar, R.K. Singh, A.R. Vaz, R. Savu, S.A. Moshkalev, ACS Appl. Mater. Interfaces 9 (2017) 8880-8890.

16. H. Fan, W. Liu, W. Shen, Chem. Eng. J. 326 (2017) 518-527.

17. K. Wang, J. Yang, J. Zhu, L. Li, Y. Liu, C. Zhang, T. Liu, J. Mater. Chem. A 5 (2017) 11236-11245.

18. S. Liu, K.H. Kim, J.M. Yun, A. Kundu, K.V. Sankar, U.M. Patil, C. Ray, S.C. Jun, J. Mater. Chem. A 5 (2017) 6292-6298.

19. J. Wang, L. Zhang, X. Liu, X. Zhang, Y. Tian, X. Liu, J. P. Zhao, Y. Li, Sci. Rep. 7 (2017) 41088.

20. H. Liang, C. Xia, Q. Jiang, A. N. Gandi, U. Schwingenschlögl, H. N. Alshareef, Nano Energy 35 (2017) 331-340.

21. G. Cheng, T. Kou, J. Zhang, C. Si, H. Gao, Z. Zhang, Nano Energy 38 (2017) 155-166.

22. Y. Zhao, L. Hu, S. Zhao, L. Wu, Adv. Funct. Mater. 26 (2016) 4085-4093.

23. N. Y, K. Guo, W. Zhang, X. Wang, M.Q. Zhu, J. Mater. Chem. A 5 (2017) 804-813.

24. H. Niu, X. Yang, H. Jiang, D. Zhou, X. Li, T. Zhang, J.Y. Liu, Q. Wang, F.Y. Qu, J. Mater. Chem. A 3 (2017) 24082-24094.

25. S. Peng, L. Li, H.B. Wu, S. Madhavi, X.W. Lou, Adv. Energy Mater. 5 (2014) 1401172.

26. J.S. Lee, D.H. Shin, J. Jun, C. Lee, J. Jang, ChemSusChem 7 (2014) 1676-1683.

27. C. Fu, A. Mahadevegowda, P.S. Grant, J. Mater. Chem. A 3 (2015) 14245-14253.

28. M. Liu, J. Sun, J. Mater. Chem. A 2 (2014) 12068-12074.

29. Q. Qu, S. Yang, X. Feng, Adv. Mater. 23 (2011) 5574-5580.

30. D. Guan, Z. Gao, W. Yang, J. Wang, Y. Yuan, B. Wang, M. Zhang, L. Liu, Mater. Sci. Eng.: B 178 (2013) 736-743.

31. H. Xia, C. Hong, B. Li, B. Zhao, Z. Lin, M. Zheng, S. V. Savilov, S. M. Aldoshin, Adv. Funct. Mater. 25 (2015) 627-635.

32. Q.X. Low, G.W. Ho, Nano Energy 5 (2014) 28-35.

33. J. Liu, M. Zheng, X. Shi, H. Zeng, H. Xia, Adv. Funct. Mater. 26 (2016) 919-930.

34. X. Tang, R. Jia, T. Zhai, H. Xia, ACS Appl. Mater. Interfaces 7 (2015) 27518-27525.

35. Y. Zeng, Y. Han, Y. Zhao, Y. Zeng, M. Yu, Y. Liu, H. Tang, Y. Tong, X. Lu, Adv. Energy Mater. 5 (2015) 1402176.

36. X. Cheng, X. Gui, Z. Lin, Y. Zheng, M. Liu, R. Zhan, Y. Zhu, Z. Tang, J. Mater. Chem. A 3 (2015) 20927-20934.

37. W. Chen, C. Xia, H. N. Alshareef, ACS Nano 8 (2014) 9531-9541.

38. W. He, C. Wang, H. Li, X. Deng, X. Xu, T. Zhai, Adv. Energy Mater. (2017) 1700983.

39. W. Fu, Y. Wang, W. Han, Z. Zhang, H. Zha, E. Xie, J. Mater. Chem. A 4 (2016) 173-182.

40. Y. Wang, C. Shen, L. Niu, R. Li, H. Guo, Y. Shi, C. Li, X. Liu, Y. Gong, J. Mater. Chem. A 4 (2016) 9977-9985.

41. S. E. Moosavifard, S. Fani, M. Rahmanian, Chem. Commun. 52 (2016) 4517-4520.

42. K. Qiu, M. Liu, Y. Luo, X. Du, J. Mater. Chem. A 5 (2017) 5820-5828.

43. S. Liu, S.C. Lee, U. Patil, I. Shackery, S. Kang, K. Zhang, J.H. Park, K.Y. Chung, S.C. Jun, J. Mater. Chem. A 5 (2017) 1043-1049.

44. J. Yang, C. Yu, X. Fan, S. Liang, S. Li, H. Huang, Z. Ling, C. Hao, J. Qiu, J. Mater. Chem. A 9 (2016) 1299-1307.

45. H. Lai, Q. Wu, J. Zhao, L. Shang, H. Li, R. Che, Z. Lyu, J. Xiong, L. Yang, X. Wang, Z. Hu, Energy Environ. Sci. 9 (2016) 2053-2060.

46. C. Guan, W. Zhao, Y. Hu, Z. Lai, X. Li, S. Sun, H. Zhang, A.K. Cheetham, J. Wang, Nanoscale Horiz. 2 (2017) 99-105.

47. L. Gao, K. Cao, H. Zhang, P. Li, J. Song, J.U. Surjadi, Y. Li, D. Sun, Y. Lu, J. Mater. Chem. A 5 (2017) 16944-16952.

48. W. Guo, C. Yu, S. Li, J. Yang, Z. Liu, C. Zhao, H. Huang, M. Zhang, X. Han, Y. Niu, J. Qiu, Small (2017) 1701288.

49. A.M. Elshahawy, C. Guan, X. Li, H. Zhang, Y. Hu, H. Wu, S.J. Pennycook, J.

Wang, Nano Energy 39 (2017) 162-171.

50. B.Y. Guan, L. Yu, X. Wang, S. Song, X.W. Lou, Adv. Mater. 29 (2017) 1605051.

51. D. Xiong, X. Wang, W. Li, L. Liu, Chem. Commun. 52 (2016) 8711-8714.

52. M. Chen, L. Shen, S. Chen, H. Wang, X. Chen, J. Wang, J. Mater. Chem. B 1 (2013) 2582-2589.

53. A. Reina, X. Jia, J. Ho, D. Nezich, H. Son, V. Bulovic, M.S. Dresselhaus, J. Kong, Nano Lett. 9 (2009) 30-35.

54. F. Yao, F. Gunes, H. Q. Ta, S. M. Lee, S. J. Chae, K.Y. Sheem, C. S. Cojocaru, S. S. Xie, Y. H. Lee, J. Am. Chem. Soc. 134 (2012) 8646-8654.

55. S. Jin, N. Li, H. Cui, C. Wang, ACS Appl. Mater. Interfaces 6 (2014) 19397-19404.

56. M. Guo, J. Balamurugan, X. Li, N. H. Kim, J. H. Lee, Small 2017, 1701275.

57. Y. Li, J. Xu, T. Feng, Q. Yao, J. Xie, H. Xia, Adv. Funct. Mater. 27 (2017) 1606728.

58. J. Chen, J. Xu, S. Zhou, N. Zhao, C. Wong, Nano Energy 21 (2016) 145-153.

59. Q. Ke, C. Guan, X. Zhang, M. Zheng, Y. Zhang, W. Cai, H. Zhang, J. Wang, Adv. Mater. 29 (2017) 1604164.